International Journal of Engineering

Journal Homepage: www.ije.ir

Numerical Study of Twin Jets Interactions using Realizable Model

K. Bouaraour*[a], N. Hebbir[b]

[a] *Laboratory of Materials, Energetic Systems Technology and Environment, University of Ghardaia, Ghardaia, Algeria*
[b] *University of Larbi ben M'hidi, Oum Elbouaghi, Algeria*

PAPER INFO

Paper history:
Received 11 August 2021
Received in revised form 27 November 2021
Accepted 13 December 2021

Keywords:
Nozzles
Turbulent Flow
Merging Point
Combined Point

ABSTRACT

In the present study, we numerically investigated the twin turbulent jets characteristics and turbulent quantities when a solid object is placed between the two nozzles. The two jets are assumed to be isothermal, incompressible and fully developed. Turbulence is modeled by the k-ε Realizable model. The set of Reynolds averaged Navier Stokes equations are solved iteratively by the Fluent software. The numerical model is validated with the experimental results available in the literature. For many Reynolds numbers, it was found that velocities and its gradients decay along the longitudinal direction. The placement of a solid object between the twin jet affects the flow structure behind nozzles due to the curvature effect of the solid object. The converging region is disappeared and the combined points axial position increases with Reynolds number. The evolution is almost linearly with an increase in Reynolds number. The effect of turbulence intensity at the exit of the nozzle is also examined. For a fixed Reynolds number, the axial combined position increases almost linearly with turbulence intensity.

***doi**: 10.5829/ije.2022.35.03c.06*

NOMENCLATURE

S	Distance betweeen nozzles centrline (m)	*U, V*	Mean velocity in the horizontal and vertical directions respectively (m/s)
K	Turbulent kinetic energy (m^2/s^2)	U_i	Mean velocity in the x_i direction (m/s)
x, y	Horizontal and vertical coordinates (m)	**Greek Symbols**	
ℓ	Turbulent length (m)	ρ	Density (kg/m^3)
g	Gravity(m/s^2)	μ	Dynamic viscosity (kg/m.s)
d	Distance between nozzles (m)	ε	Dissipation rate of K (m^2/s^3)
P	Pressure (Pa)	ν	Kinematic viscosity (m^2/s)
Re	Reynolds number	**Subscripts**	
P_K	Turbulent generating source in K equation ($kg/m.s^3$)	0	Related to the outlet of nozzles
u_i	Turbulent fluctuation in x_i the direction (m/s)	t	turbulent

1. INTRODUCTION

Two jets interactions have many practical engineering applications as in the injection systems, burners, mixing and drying processes. Behind the nozzles, interaction between the two jets passes throw many steps until it merge to a single flow. Tanaka [1, 2] has found that flow field of twin jets interaction is characterized by three distinct zones: The converging zone, the merging zone and the combined zone. The converging zone is located between nozzle exit and the point where the inner shear layers of the jets merge. The location where the velocity at the symmetry plane reaches its maximum is called the combined point and denotes that the merging region ends and the combined region begins [3, 4]. The combined zone is downstream of the combined point where the two jets begin to resemble a self-similar single jet. The schematic of the flow field is given by Figure 1 [5]. When Reynolds number is greater than 2000, jets become turbulent as experimentally indicated by Kwon and Seo [6]. Inorder to increase the mixing and combustion efficiencies, Ali et al. [7] have investigated numerically

*Corresponding Author Institutional Email: bouaraourk@yahoo.fr
(B Kamel)

Please cite this article as: K. Bouaraour, N. Hebbir, Numerical Study of Twin Jets Interactions using Realizable Model, ***International Journal of Engineering, Transactions C: Aspects*** Vol. 35, No. 03, (2022) 544-551

the flame holding capability of a supersonic combustor by varying the distance of injector position. Results show that for moderate distance of injector position, large and elongated upstream recirculation can evolve which might be activated as a good flame holder.

Three different numerical models were used to investigate the interaction of twin plane parallel jets [5]. Results showed that position of merging and combined points are strongly affected by the velocity ratio and nozzles spacing. Correlations between the merge and combined points position are also made.

Many experimental and numerical studies focused on the interference region between the twin jets, by varying velocity ratio of the two jets [8], or by varying some geometrical parameters, such as nozzles spacing (S/d) [9-11]. Also, effect of different parameters on the flow structure is studied by Abdel-rahman [12], particularly initial and boundary conditions. Pandey and Kumar [13] studied the effects of pressure ratio and Mach numbers on the flow field along with the flow and lateral directions were examined. The main finding results was that the width of the twin jets spreads linearly downstream and grows with nozzles spacing and the merging length of the two jets can be increased either by reducing nozzles spacing or increasing Mach number. More recently, a numerical study focused on the characteristics of self-oscillating twin jets using the Reynolds Stress Turbulence Model [14]. Many nozzles spacing are used with a fixed Reynolds number (Re = 27000).

Numerical results show that for nozzle spacings of up to four, the two jets merge downstream and oscillate as an equivalent single jet, but for higher nozzle spacing, the two jets do not merge but oscillate separately. Nozzle shape is also examined, but it does not significantly affect the jet decay. In addition, twin oscillating jets produce higher spread and turbulence intensity over a wider area, which may be beneficial for cooling of hot devices in industrial applications.

In order to investigate the spatial evolution of a dual-plane jet flow and to contribute to a better understanding of the dual-plane jet flow, DNS was performed by Hao et al. [15]. For a fixed nozzle spacing, the combination of transport, convection, production, pressure, and viscous dissipation is well explained in the different flow regions. It is demonstrated that even in the highly intermittent region, the characteristics of small-scale motions are already close to the fully developed flow.

CFD software was used to solve a three-dimensional flow situation [16].The studied configuration is formed by nine impinging jets in a square array used to cool a plate maintained at constant heat flux. Numerical code has been executed using three k-ε models and the SST k-ω model. Numerical results show that this last has been noticed to be in maximum agreement with the experimental results, and the local heat transfer coefficient has been declining with the rise in separation distance.

In spite of numerous experimental and numerical investigations of turbulent jet flows, few studies focused on the investigation of flow characteristics when an obstacle is placed between the two jets, because of the difficulty of accurately predicting the interaction of the flow structures.

The aim of this study is to investigate numerically the effect of surface curvature when placing different solids bodies between the two parallel jets. The Fluent software was used to solve the governing dynamic equations, due to its efficiency to provide reasonable solutions in many earlier studies [17-20]. Turbulent velocities and turbulent fields were examined and compared with the configuration without obstacle.

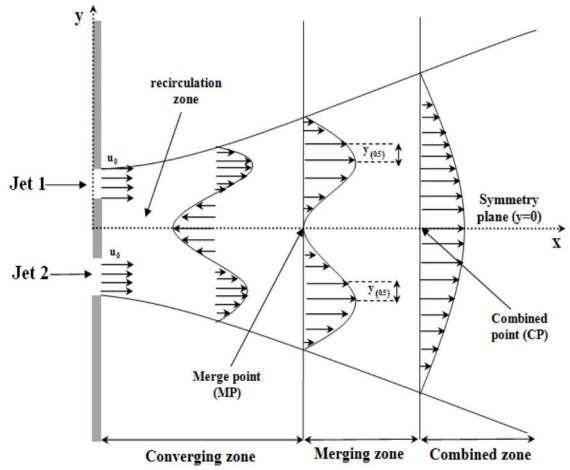

Figure 1. Schematic diagram of dual jet

2. GEOMETRICAL CONFIGURATION

The studied geometrical configurations are shown in Figure 2. We consider two parallel turbulent jets where the distance between nozzles centerline is **S** and nozzles width is **d,** where **S/d=6**. Dimensions adopted in the transverse and longitudinal directions are respectively **100d** and **200d**. Configurations are respectively denoted by A and B. The Configuration B is characterized by the placement of a a half-circle object between nozzles compared to the configuration A.

The working fluid is air, which is assumed to be incompressible and with constant thermo-physical properties. Reynolds numbers based on the inlet velocity and the nozzle width varied from 2000 to 8000. Turbulence intensity distribution at the nozzles exit section is uniform and takes different values (1, 3 and 6%).

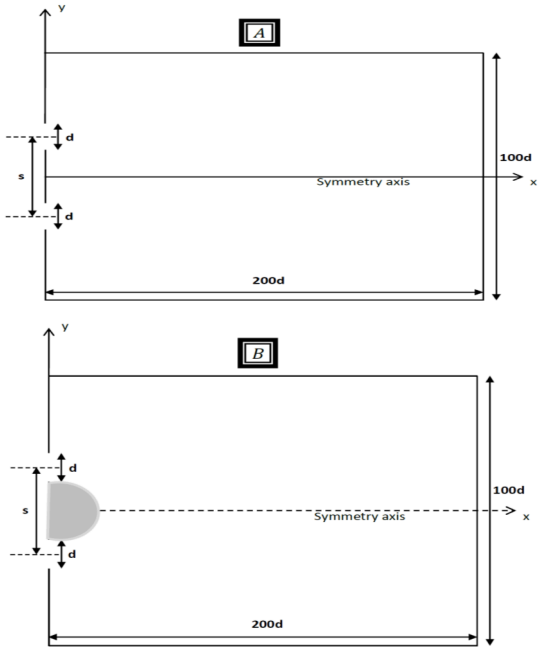

Figure 2. Geometrical configurations

3. GOVERNING EQUATIONS AND BOUNDARY CONDITIONS

The governing equations for turbulent flow are described mathematically by the Reynolds averaged Navier-Stokes equations (RANS). The flow is assumed to be steady, two dimensional, and fully developed at the exit of the nozzles. Turbulence intensity at the exit of the nozzles varies from 1 to 6%. The RANS equations can be written as follows:

$$\frac{\partial U_i}{\partial X_i} = 0 \tag{1}$$

$$\frac{\partial (U_i U_j)}{\partial X_j} = -\frac{1}{\rho}\frac{\partial P}{\partial X_i} + \frac{\partial}{\partial X_j}\left[\nu \frac{\partial U_i}{\partial X_j} - \overline{u_i u_j}\right] \tag{2}$$

Where turbulence stress is approximated as:

$$\overline{u_i u_j} = \frac{2}{3}\delta_{ij}K - \nu_t\left(\frac{\partial U_i}{\partial X_j} + \frac{\partial U_j}{\partial X_i}\right) \tag{3}$$

The Kronecker delta is given by δ_{ij} =1 if (i=j) and δ_{ij} =0 if (i ≠ j), and the turbulence viscosity is defined as:

$$\nu_t = C_\mu \frac{K^2}{\varepsilon} \tag{4}$$

Turbulence is modeled with the Realizable model [21] based on the k-ε model derived from the stationary Reynolds average Navier-Stokes equations. The Realizable model is an eddy-viscosity model similar to the standard k-ε model, which perform better results than the standard k-ε model when flow separation and recirculation occur. The concept of realizability introduced by Lumley signifies that the model must respect asymptotic situations. For exemple K and ε must never be negative. This model seems well adapted to circular jets, boundary layers with strong adverse pressure gradients, flows with strong curvature and vortex flows.

$$\frac{\partial (\rho U_i K)}{\partial X_i} = \frac{\partial}{\partial X_i}\left(\mu + \frac{\mu_t}{\sigma_K}\frac{\partial K}{\partial X_i}\right) + P_K - \rho\varepsilon \tag{5}$$

$$\frac{\partial (\rho U_i \varepsilon)}{\partial X_i} = \frac{\partial}{\partial X_i}\left(\mu + \frac{\mu_t}{\sigma_\varepsilon}\frac{\partial \varepsilon}{\partial X_i}\right) + C_{\varepsilon 1}\frac{\varepsilon}{K}P_K - \rho C_{\varepsilon 2}\frac{\varepsilon^2}{K+\sqrt{\nu\varepsilon}} \tag{6}$$

The analytical derivation results in a model with constants that are different from those employed in the standard k- ε model, where P_k is the sheer production of turbulence kinetic energy.

$$C_\mu = \frac{1}{A_0 + A_s U^* \frac{K}{\varepsilon}} \tag{7}$$

$$A_s = \sqrt{6}cos\emptyset \tag{8}$$

with:

$$\emptyset = \frac{1}{3}cos^{-1}(\sqrt{6}W) \tag{9}$$

$$W = S_{ij}S_{jk}S_{ki}/\tilde{S} \tag{10}$$

And the strain tensor is defined as:

$$S_{ij} = \frac{1}{2}\left(\frac{\partial U_i}{\partial X_j} + \frac{\partial U_j}{\partial X_i}\right) \tag{11}$$

$$\tilde{S} = \sqrt{S_{ij}S_{ji}} \tag{12}$$

$$U^* = \sqrt{S_{ij}S_{jk} + \tilde{\Omega}_{ij}\tilde{\Omega}_{ij}} \tag{13}$$

$$\tilde{\Omega}_{ij} = \Omega_{ij} - 2\epsilon_{ij}\omega_k \tag{14}$$

$$\Omega_{ij} = \overline{\Omega_{ij}} - \epsilon_{ij}\omega_k \tag{15}$$

Where ω_k is the angular velocity and $\overline{\Omega_{ij}}$ is the rotation coefficient tensor. The constants of this model are presented in Table 1.

TABLE 1. Constants of the Realizable k-ε model

A_0	$C_{\square 1}$	$C_{\square 2}$	σ_k	σ_ε
4.04	1.42	1.68	1	1.2

The boundary conditions for the considered problem can be expressed as:

- The velocity at the exit of the nozzles is: $U=U_0$ and $V_0=0$.
- Turbulent kinetic energy and its dissipation rate at the exit of the nozzles are respectively: $K_0=1.5(U_0I_0)^2$ and $\varepsilon_0=K_0^{1.5}/\ell$. ℓ: is a turbulent length scale (ℓ=d/10 m) and I_0 is the inlet turbulent intensity.
- At the gap of the outlet, gradients of all variables in the y- direction are set to zero.
- The velocity boundary conditions were fixed to zero over the solid walls.
- Symmetry condition is applied on the horizontal axis between nozzles.

4. NUMERICAL METHODS

The governing equations are discretized using finite volumes schemes and the solver is the commercial CFD code FLUENT 6.3.26. The velocity components are calculated at a staggered grid while the scalar variables are calculated at the main grid (not staggered). For coupling of mass and momentum equations, SIMPLEC algorithm is used [22]. The discretization of pressure is based on the PRESTO! scheme. The Green-Gauss cell based scheme is used for gradient discretization. Second-order upwind central differencing is used for flow terms, while first order upwind central differencing is used for turbulent kinetic energy and turbulent dissipation rate. The convergence criterion was taken 10^{-4} for the normalized residual of each equation. We have used relaxation factors of 0.7 for velocities, 0.8 for turbulent quantities and 0.3 for the pressure.

5. VALIDATION AND GRID INDEPENDENCE

To validate the mathematical model and numerical methods, it has been tested with the experimental results reported by Anderson and Spall [23]. The configuration of Anderson and Spall is like the configuration **A** with a nozzles spacing (S/d =9). Dimensions along the transverse and longitudinal directions are 100d and 150d, respectively. The Reynolds number was set at 6000 and the turbulent intensity at the outlet of the nozzles was 3.6%. Numerical simulations are obtained with non-uniform meshes of different grid sizes: 450 × 168, 480 × 252 and 600 × 336 (see Figure 3). The deviation between the two last meshes was less than 1.23% for the maximum vertical velocity and less than 2% for the maximum turbulent kinetic energy.

The maximum turbulent viscosity deviation reaches 0.95%, so mesh 3 was adopted (see Table 2).

Our numerical results show a good agreement with the experimental data, as indicated in Figure 4.

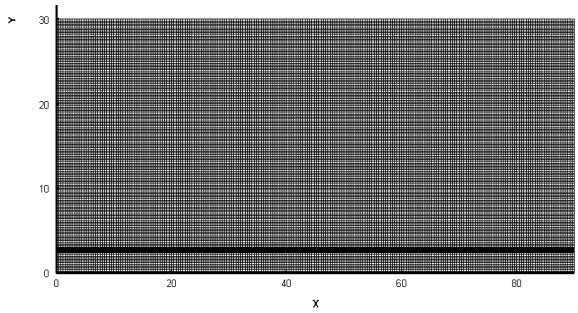

Figure 3. Computational grid structure

TABLE 2. Deviation between meshes

	Mesh1	Mesh 2	Mesh 3
V_{max} (m/s)	1.51	1.615	1.63
K_{max} (m²/s)	24.28	27.73	28.27
$\nu_{t\ max}$ (m²/s³)	1.789	1.772	1.789

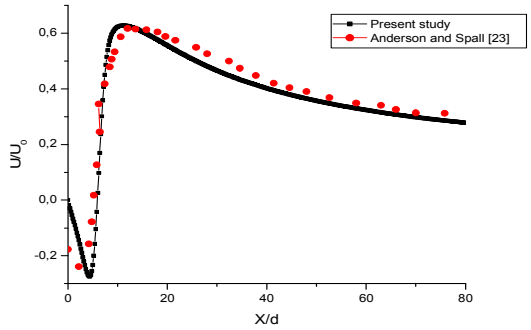

Figure 4. Axial mean velocity distribution along the symmetry axis for S/d=9

6. RESULTS AND DISCUSSION

We Considered two plan jets (S/d=6), where the Reynolds number was varied from 2000 to 8000. Turbulence intensity at the inlet of nozzles was varied from 1 to 6%. Figure 5 shows the evolution of the axial mean velocity on the symmetry axis (y=0) for different Reynolds numbers. The merging point is determined by the stagnation point, where the mean velocity is zero in the symmetry axis.

6. 1. Configuration A The mean axial velocity distribution at the symmetry axis is indicated in Figure 5. Since the velocity ratio is one (the same exit velocity for the two nozzles), the axial location of merge and combined points always occurs in the symmetry axis (y=0) as mentioned by Lin and Sheu [24], and by Anderson and Spall [23].

For a fixed Reynolds number, a very slight effect has been detected on the velocity profiles only for high Reynolds numbers, as indicated in Figure 6.

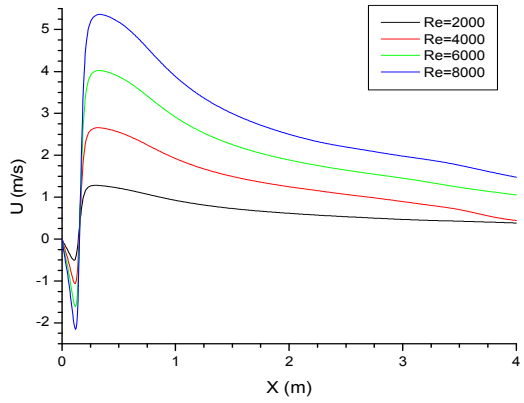

Figure 5. Axial mean velocity distribution along the symmetry axis for I_0=1%

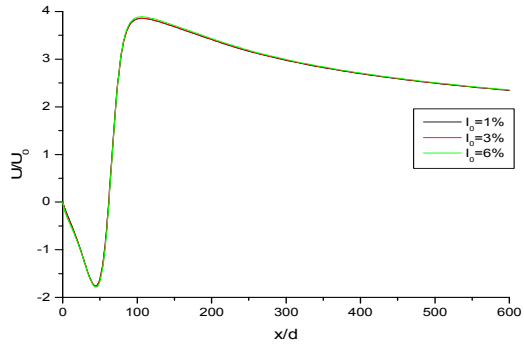

(a)

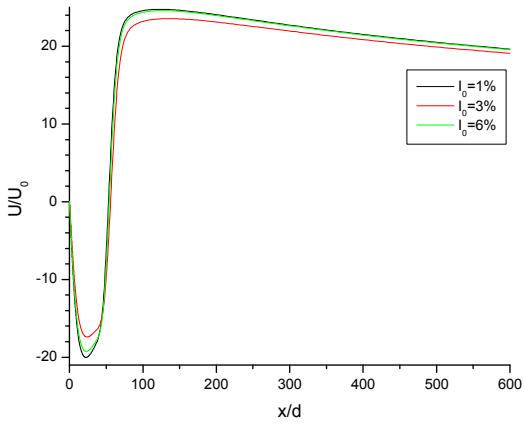

(b)

Figure 6. Intensity effect along the symmetry axis for:(a) Re=2000,(b) Re=8000

6. 2. Configuration B For the chosen Reynolds numbers, the figure below shows the evolution of the axial velocity at the symmetry axis for different turbulence intensities.

From Figure 7, we can see that velocity profiles maintain their self-similarity behaviour. We can also see that the combined point axial position increases with Reynolds number. The locations of combined points are illustrated in Table 3.

We have varied the intensity of the turbulence at the exit of the nozzles from 1 to 6%. For a fixed Reynolds number (Re=2000), no significant effect is observed on

I_0=1 %

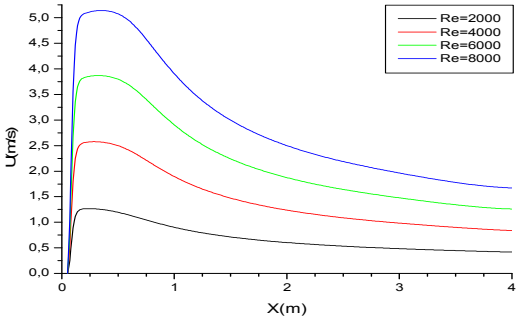

I_0=3%

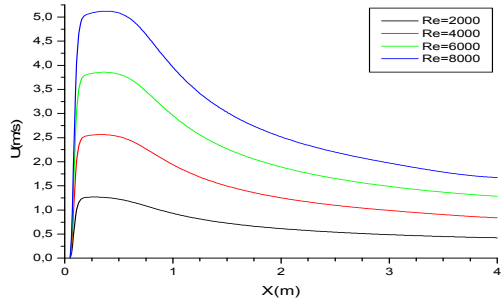

I_0=6%

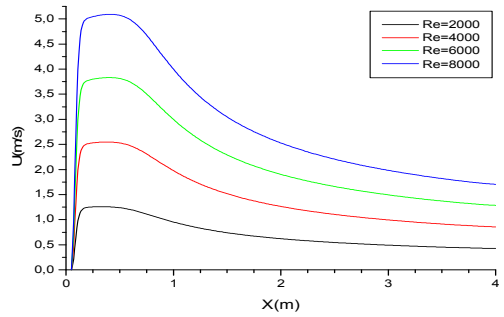

Figure 7. Axial mean velocity distribution along the symmetry axis

the mean axial velocity as indicated in Figure 8. The same behaviour is observed for the other Reynolds numbers.

It's noted that for a fixed spacing, combined point position is affected by turbulence intensity at the exit of nozzles. Combined point axial location increases almost linearly with turbulence intensity.

For a given turbulence intensity (3%), the x-velocity contours are given in Figure 9 for different Reynolds numbers. At the nozzle exit, high velocities lead to entrainment of fluid in the shear layers of the jets. Entrainment rates in the region between the two jets are high, which results in a region of very low pressure between the jets.

The velocities and its gradients decay along x-axis. Due to the effect of entrainment in the shear layer, the velocity between two jets increases with x-axis.

The Figure 10 demonstrates the vectors of mean velocity for Re=8000 and for I_0=1%. It is observed that the width of twin jets increased further downstream. The region from nozzle outlets to the merge point is the merge region, which is characterized by reverse flow in this region.

From merge point inner shear layers of the jets begin to merge and are characterized as velocity is zero. The merge point is also characterized by high pressure

TABLE 3. Locations of combined points for different Reynolds numbers

	X_{CP}(m) for I_0=1%	X_{CP}(m) for I_0=3%	X_{CP}(m) for I_0=6%
Re=2000	0.23	0.27	0.335
Re=4000	0.285	0.33	0.38
Re=6000	0.325	0.36	0.40
Re=8000	0.35	0.38	0.41

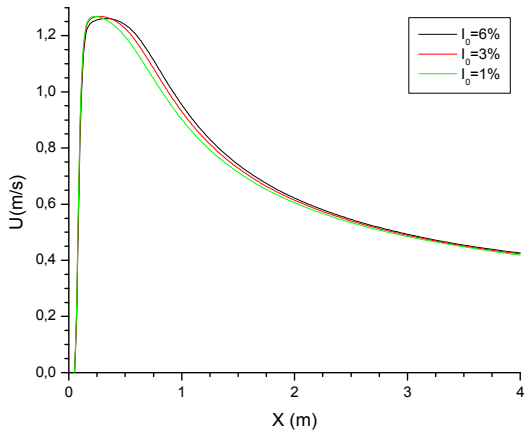

Figure 8. Axial mean velocity distribution along the symmetry axis for Re=2000.

Re=2000

Re=4000

Re=6000

Re=8000

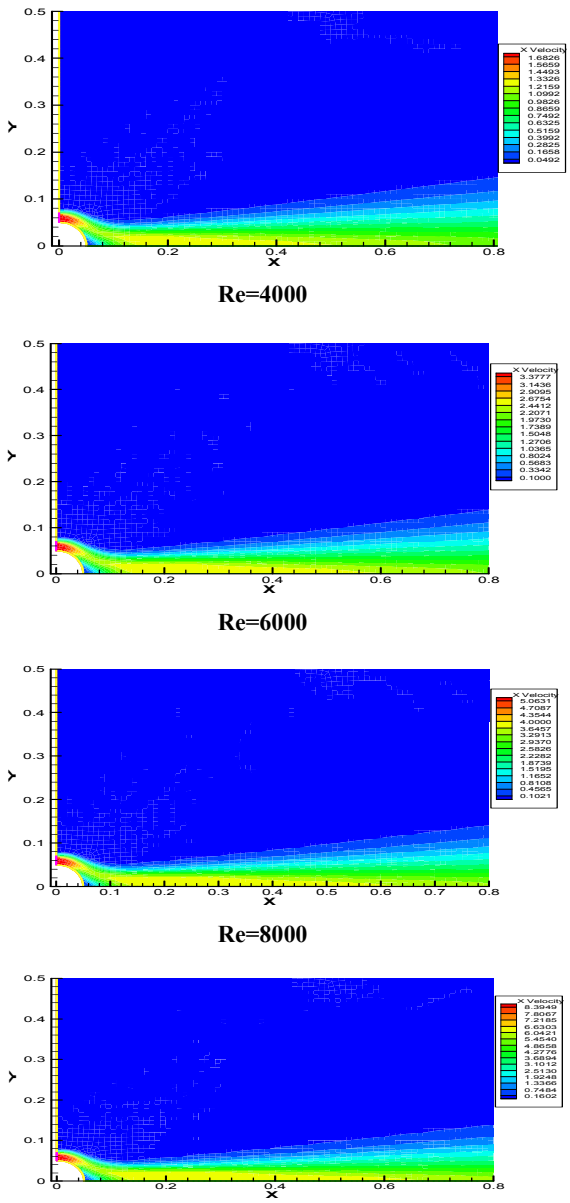

Figure 9. Axial velocity contours for configuration B

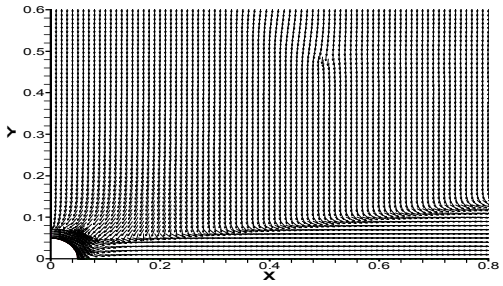

Figure 10. Vectors of mean velocity for Re=8000 and I_0=1%.

7. CONCLUSION

In this study, we have investigated numerically the effect of placing a solid object between nozzles in twin turbulent jets. The Realizable based k-ε model is used to describe turbulence, and the commercial Fluent 6.3.26 code is used for the resolution of the transport equations. The numerical model is validated with the experimental data available in the literature. Two different configurations have been tested:

The configuration **A,** which is characterised by the presence of two similar nozzles, where the nozzles width is **d** and the nozzles centerlines is **S (S/d=6)**. The configuration **B** differs from the first configuration by the placement of a solid object between nozzles. The Reynolds number at the exit of nozzles varies between Re=2000 and Re=8000. The flow structure for configuration B, is strongly affected behind nozzles compared to the configuration A. Due to the curvature effect of the solid object, the converging region is disappeared and the combined points axial position is strongly affected. The evolution is almost linearly with the increase of the Reynolds number. Combined points axial positions increases with Reynolds number and velocities and their gradients decay along the longitudinal direction. The effect of the turbulence intensity at the exit of the nozzle is examined. Three values are tested: I_0=1%, I_0=3 and I_0=6%. For a fixed Reynolds number, the axial combined position increases almost linearly with turbulence intensity.

8. REFERENCES

1. Tanaka, E.J.B.o.J., "The interference of two-dimensional parallel jets: 1st report, experiments on dual jet", ***Bulletin JSME***, Vol. 13, No. 56, (1970), 272-280, doi: 10.1299/jsme1958.13.272
2. Tanaka, E.J.B.o.J., "2nd report, experiments on the combined flow of dual jet", ***Bulletin JSME***, Vol. 17, (1974), 920-927, doi: 10.1299/jsme1958.17.920
3. Fairuzov, Y.V. and Arvizu, H.J.J.H.T., "Numerical solution for transient conjugate two-phase heat transfer with heat generation in the pipe wall", ***Journal of Heat Transfer***, Vol. 124, No. 6, (2002), 1213-1218, doi: 10.1115/1.1470170
4. Tenchine, D. and Moro, J.P., "Experimental and numerical study of coaxial jets", Vol. 3, (1997), 1381–1387, doi: 10.1080/18811248.1998.9733851
5. Mohammadi, M., Samadi, S. and Najafpour Darzi, G.J.I.J.o.E., "Production of single cell protein from sugarcane bagasse by saccharomyces cerevisiae in tray bioreactor", ***International journal of engineering, Transactions A: Basics***, Vol. 29, No. 8, (2016), 1029-1036, doi: 10.5829/idosi.ije.2016.29.10a.13
6. Kwon, S.J. and Seo, I.W.J.E.i.f., "Reynolds number effects on the behavior of a non-buoyant round jet", ***Experiments in Fluids***, Vol. 38, No. 6, (2005), 801-812, doi: 10.1007/s00348-005-0976-6
7. Ali, M., Ahmed, S. and SADR, A.A., "A numerical study on mixing of transverse injection in supersonic combustor", ***International journal of engineering, Transactions A: Basics***, (2004).
8. Elbanna, H. and Sabbagh, J.J.A.j., "Interaction of two nonequal plane parallel jets", ***AIAA Journal***, Vol. 25, No. 1, (1987), 12-13, doi: 10.2514/3.9571
9. Nasr, A. and Lai, J.J.E.i.f., "Two parallel plane jets: Mean flow and effects of acoustic excitation", ***Experiments in Fluids***, Vol. 22, No. 3, (1997), 251-260, doi: 10.1007/s003480050044
10. Elbanna, H., Gahin, S. and Rashed, M.J.A.j., "Investigation of two plane parallel jets", ***AIAA Journal***, Vol. 21, No. 7, (1983), 986-991, doi: 10.2514/3.8187
11. Elbanna, H., Sabbagh, J. and Rashed, M.J.A.j., "Interception of two equal turbulent jets", ***AIAA Journal***, Vol. 23, No. 7, (1985), 985-986, doi: 10.2514/3.9027
12. Abdel-Rahman, A.J.W.t.o.F.M., "A review of effects of initial and boundary conditions on turbulent jets", ***WSEAS Transactions on Fluid Mechanics***, Vol. 4, No. 5, (2010), 257-275, doi:
13. Pandey, K., Kumar, V.J.I.J.o.E.S. and Development, "Cfd analysis of twin jet flow at mach 1.74 with fluent software", ***International Journal of Environmental Science and Development***, Vol. 1, No. 3, (2010), 423-428, doi: 10.7763/IJESD.2010.V1.81
14. Mosavati, M., Balachandar, R. and Barron, R.J.P.o.F., "Characteristics of self-oscillating twin jets", ***Physics of Fluids 33***, Vol. 33, No. 3, (2021), 035129, doi: 10.1063/5.0033869
15. Hao, K., Tian, A., Zhou, Y.J.I.J.o.H. and Flow, F., "Characteristics of small-scale motions in a dual-plane jet flow", ***International Journal of Heat and Fluid Flow***, Vol. 91, (2021), 108851, doi: 10.1016/j.ijheatfluidflow.2021.108851
16. Singh, P., Grover, N.K., Agarwal, V., Sharma, S., Singh, J., Sadeghzadeh, M. and Issakhov, A.J.M.P.i.E., "Computational fluid dynamics analysis of impingement heat transfer in an inline array of multiple jets", ***Mathematical Problems in Engineering***, Vol. 2021, (2021), doi: 10.1155/2021/6668942
17. Pandey, K., Kumar, V.J.I.J.o.C.E. and Applications, "Cfd analysis of four jet flow at mach 1.74 with fluent software", ***International Journal of chemical engineering and applications***, Vol. 1, No. 4, (2010), 302, doi: 10.7763/IJCEA.2010.V1.53
18. Zheng, X., Jian, X., Wei, J. and Wenzheng, D.J.I.J.o.A.E., "Numerical and experimental investigation of near-field mixing in parallel dual round jets", ***International Journal of Aerospace Engineering***, Vol. 2016, (2016), doi: 10.1155/2016/7935101
19. Boussoufi, M., Sabeur-Bendehina, A., El Ganaoui, M., Morsli, S. and Ouadha, A.J.E.P., "Numerical simulation of the flow field analysis in the mixing twin jets", ***Energy Procedia***, Vol. 139, (2017), 161-166, doi: 10.1016/ j.egypro.2017.1.190
20. Jafarmadar, S.J.I.J.o.E., "The effects of pressure difference in nozzle's two phase flow on the quality of exhaust mixture", ***International Journal of Engineering-Transactions B: Applications***, Vol. 26, No. 5, (2013), 553-562, doi: 10.5829/idosi.ije.2013.26.05b.12
21. Shih, T.-H.J.C. and Fluids, "J. A new _< k-ε> eddy-viscosity model for high reynolds number turbulent flows-model development and validation", ***Computers and Fluids***, Vol. 24, (1995), 227, doi: 10.1016/0045-7930(94)00032-T
22. Baliga, B. and Patankar, S.J.N.H.T., "A new finite-element formulation for convection-diffusion problems", Vol. 3, No. 4, (1980), 393-409,
23. Anderson, E.A. and Spall, R.E.J.J.F.E., "Experimental and numerical investigation of two-dimensional parallel jets", ***Journal of Fluids Engineering***, Vol. 123, No. 2, (2001), 401-406, doi: 10.1115/1.1363701
24. Lin, Y. and Sheu, M.J.A.j., "Interaction of parallel turbulent plane jets", ***AIAA Journal***, Vol. 29, No. 9, (1991), 1372-1373, doi: 10.2514/3.10749

Persian Abstract

چکیده

در مطالعه حاضر، ما ویژگی‌های جت‌های آشفته دوقلو و مقادیر آشفته را زمانی که یک جسم جامد بین دو نازل قرار می‌گیرد، بررسی کردیم. فرض می شود که دو جت همدما، تراکم ناپذیر و کاملاً توسعه یافته هستند. آشفتگی با مدل Realizable k-ε مدل‌سازی می‌شود. مجموعه معادلات میانگین ناویر استوکس رینولدز به صورت تکراری توسط نرم افزار فلوئنت حل می شود. مدل عددی با نتایج تجربی موجود در ادبیات تایید شده است. برای بسیاری از اعداد رینولدز، مشخص شد که سرعت ها و گرادیان های آن در امتداد جهت طولی کاهش می یابند. قرار گرفتن یک جسم جامد بین جت دوقلو بر ساختار جریان در پشت نازل ها به دلیل اثر انحنای جسم جامد تأثیر می گذارد. منطقه همگرا ناپدید می شود و موقعیت محوری نقاط ترکیبی با عدد رینولدز افزایش می یابد. تکامل تقریباً خطی با افزایش عدد رینولدز است. اثر شدت تلاطم در خروجی نازل نیز مورد بررسی قرار می گیرد. برای یک عدد رینولدز ثابت، موقعیت ترکیبی محوری تقریباً به صورت خطی با شدت تلاطم افزایش می‌یابد.